



The North African Journal of Scientific Publishing (NAJSP)

مجلة شمال إفريقيا للنشر العلمي (NAJSP)

E-ISSN: 2959-4820

Volume 4, Issue 2, 2026

Page No: 256-264

Website: <https://najsp.com/index.php/home/index>



Directory of Online Libyan Journals

SJIFactor 2024: 5.49

معامل التأثير العربي (AIF) :2025 0.69

ISI 2024: 0.696

Numerical study of Structural Behavior and Moment Redistribution in Continuous FRP-Reinforced Concrete Beams

Mohamed Elarbi Mahroug^{1*}, Amina Yousif Alharan²

^{1,2}Faculty of Engineering, Sabratha University, Sabratha, Libya.

دراسة عددية للسلوك الإنشائي وإعادة توزيع العزوم في الكمرات الخرسانية المستمرة المسلحة بألياف (FRP)

محمد العربي المحروق^{1*}، أمينة يوسف الحران²
^{1,2}كلية الهندسة، جامعة صبراتة، صبراتة، ليبيا

*Corresponding author: mohamed.elmahroug@sabu.edu.ly

Received: March 02, 2026

Accepted: April 20, 2026

Published: April 30, 2026

Copyright: © 2026 by the authors. Submitted for possible open access publication under the terms and conditions of the Creative Commons Attribution (CC BY) license (<https://creativecommons.org/licenses/by/4.0/>).

Abstract:

This study investigates the structural behavior and moment redistribution capacity of continuous reinforced concrete beams reinforced with Fiber Reinforced Polymer (FRP) bars through analytical and numerical approaches. The use of FRP reinforcement has gained significant attention in recent years due to its high corrosion resistance, high tensile strength, and suitability for aggressive environmental conditions where conventional steel reinforcement suffers from durability problems. Unlike steel reinforcement, FRP bars exhibit linear elastic behavior up to failure without yielding, resulting in different flexural and redistribution characteristics in statically indeterminate structures. The present research focuses on evaluating the influence of reinforcement ratio on the flexural response and moment redistribution behavior of continuous FRP-reinforced concrete beams. A nonlinear numerical model was developed to simulate the structural behavior of the beams considering nonlinear material behavior. The analytical and numerical results were used to assess the redistribution of internal moments and the overall load-carrying performance of the beams. The results indicate that moment redistribution can occur in continuous FRP-reinforced concrete beams despite the absence of yielding in FRP reinforcement. The redistribution behavior was found to be strongly influenced by reinforcement ratio, concrete strength, and beam stiffness. Beams with lower reinforcement ratios exhibited greater redistribution capacity due to increased cracking and stiffness reduction, whereas higher reinforcement ratios resulted in reduced redistribution behavior. The study demonstrates that nonlinear concrete behavior and stiffness degradation play a major role in the redistribution mechanism of FRP-reinforced continuous beams. The findings of this study contribute to a better understanding of the structural behavior of continuous FRP-reinforced concrete beams and provide useful insights for the development of reliable design approaches and future code provisions for FRP-reinforced concrete structures.

Keywords: Fiber Reinforced Polymer (FRP), Continuous Concrete Beams, Moment Redistribution, GFRP, CFRP, Nonlinear Analysis, Reinforced Concrete, Flexural Behavior.

المخلص:

تتناول هذه الدراسة السلوك الإنشائي وقدرة إعادة توزيع العزوم في الكمرات الخرسانية المستمرة المسلحة بألياف البوليمر (FRP) من خلال الطرق التحليلية والعديدية. وقد حظي استخدام تسليح أسياخ الفايبر (FRP) باهتمام متزايد خلال السنوات الأخيرة نظرًا لمقاومته العالية للتآكل، وامتلاكه مقاومة شد مرتفعة، وملاءمته للبيئات القاسية التي تعاني فيها قضبان التسليح الفولاذية التقليدية من مشكلات المتانة والاستدامة. وعلى عكس التسليح الفولاذي، تُظهر أسياخ الفايبر سلوكًا مرئيًا خطيًا حتى الانهيار دون حدوث خضوع، مما يؤدي إلى خصائص مختلفة في الانحناء وإعادة توزيع العزوم في المنشآت غير المحددة استاتيكيًا. يركز البحث الحالي على تقييم تأثير نسبة التسليح على الاستجابة الانحنائية وسلوك إعادة توزيع العزوم في الكمرات الخرسانية المستمرة المسلحة بألياف (FRP). وقد تم تطوير نموذج عددي لاخطي لمحاكاة السلوك الإنشائي للكمرات الخرسانية مع الأخذ في الاعتبار السلوك اللاخطي للمواد. واستخدمت النتائج التحليلية والعديدية لتقييم إعادة توزيع العزوم الداخلية والأداء العام لتحمل الأحمال للكمرات. أظهرت النتائج إمكانية حدوث إعادة توزيع للعزوم في الكمرات الخرسانية المستمرة المسلحة بألياف (FRP) على الرغم من عدم وجود خضوع في تسليح الألياف (FRP) كما تبين أن سلوك إعادة التوزيع يتأثر بشكل كبير بنسبة التسليح، ومقاومة الخرسانة، وصلابة الكمرات. فقد أظهرت الكمرات ذات نسب التسليح المنخفضة قدرة أكبر على إعادة توزيع العزوم نتيجة زيادة التشقق وانخفاض الصلابة، في حين أدت نسب التسليح المرتفعة إلى تقليل سلوك إعادة التوزيع. وتوضح الدراسة أن السلوك اللاخطي للخرسانة وتدهور الصلابة يلعبان دورًا رئيسيًا في آلية إعادة توزيع العزوم في الكمرات المستمرة المسلحة بألياف (FRP) وتسهم نتائج هذه الدراسة في تحسين فهم السلوك الإنشائي للكمرات الخرسانية المستمرة المسلحة بألياف (FRP)، كما توفر مؤشرات مفيدة لتطوير أساليب تصميم موثوقة ومتطلبات مستقبلية في الكودات الخاصة بالمنشآت الخرسانية المسلحة بألياف (FRP).

الكلمات المفتاحية: البوليمرات المسلحة بالألياف (FRP)، الكمرات الخرسانية المستمرة، إعادة توزيع العزوم، GFRP، CFRP، التحليل اللاخطي، الخرسانة المسلحة، السلوك الإنحنائي.

Introduction:

Reinforced concrete (RC) structures are among the most commonly used structural systems in civil engineering because of their strength, durability, versatility, and economic efficiency. However, the durability of conventional steel-reinforced concrete structures is significantly influenced by the corrosion of steel reinforcement, particularly in aggressive environments such as marine regions, industrial areas, and structures exposed to de-icing salts. Corrosion of reinforcing steel results in cracking and spalling of concrete, reduction in structural capacity, increased maintenance costs, and shortened service life of infrastructure systems (Mehta and Monteiro, 2014; Neville, 2011). Consequently, extensive research has focused on developing alternative reinforcing materials capable of overcoming corrosion-related deterioration problems. Fiber Reinforced Polymer (FRP) bars have emerged as a promising alternative to conventional steel reinforcement due to their non-corrosive characteristics, high tensile strength, lightweight properties, and excellent resistance to chemical and environmental attacks (ACI 440.1R-15, 2015; Benmokrane et al., 2002). In recent decades, FRP reinforcement has been increasingly utilized in civil engineering structures, especially in harsh environmental conditions where durability is a major concern. Among the different types of FRP reinforcement, Glass Fiber Reinforced Polymer (GFRP) and Carbon Fiber Reinforced Polymer (CFRP) bars have attracted considerable attention because of their favorable mechanical properties and practical applicability in reinforced concrete structures (Bank, 2006).

Numerous experimental and analytical studies have investigated the flexural behavior of simply supported FRP-reinforced concrete beams, demonstrating the effectiveness of FRP bars in improving corrosion resistance and structural durability (El-Salakawy et al., 2003; Toutanji and Saafi, 2000). Nevertheless, relatively limited research has addressed the behavior of statically indeterminate FRP-reinforced concrete members such as continuous beams. In continuous reinforced concrete beams, moment redistribution is an important structural phenomenon that directly affects ductility, safety, and load-carrying capacity. In steel-reinforced concrete members, moment redistribution mainly occurs due to steel yielding and the formation of plastic hinges. However, FRP reinforcement exhibits a linear elastic behavior up to failure without yielding, making the redistribution mechanism fundamentally different from that of conventional steel-reinforced members (Grace et al., 1998; Ospina and Gross, 2005). Despite the absence of yielding in FRP bars, previous studies have shown that moment redistribution may still occur in FRP-reinforced continuous beams due to concrete cracking, stiffness degradation, nonlinear concrete behavior, and bond interaction between FRP reinforcement and concrete (Kara et al. 2013; Gravina and Smith, 2008; Habeeb and Ashour, 2008). Therefore, understanding the redistribution behavior of FRP-reinforced continuous beams is essential for developing reliable design methodologies and expanding the practical applications of FRP reinforcement in modern structural engineering. The present study investigates the structural behavior and moment redistribution capacity of continuous concrete beams reinforced with GFRP and CFRP

bars using analytical and numerical approaches. The study also examines the influence of reinforcement ratio and transverse reinforcement characteristics on the redistribution behavior and flexural performance of continuous GFRP and CFRP-reinforced concrete beams.

Numerical Model Concept (Mahroug, 2026):

1. Computational Frame:

The proposed computational model is based on Artificial Neural Network (ANN) principles combined with a sectional analysis approach to capture the nonlinear structural behavior of reinforced concrete beams.

- The beam cross-section is divided into a large number of horizontal slices (discretization).
- The Bisection Method is used to determine the neutral axis depth (c) accurately, which is considered a key step in nonlinear analysis of reinforced concrete sections.
- Stress and strain in each slice are calculated using nonlinear stress–strain relationships for concrete and reinforcement materials.

2. Numerical Data Generation and Processing:

Data for the model were prepared by simulating the beam cross-section with approximately 10,000 horizontals:

- Strain in each slice was computed assuming that plane sections remain plane after bending.
- Nonlinear material behavior of concrete and FRP reinforcement was used to calculate stress in each slice.
- Internal moment was obtained by summing the contribution of all slices relative to the neutral axis.

3. Python Implementation of the Computational Model:

The computational procedure is implemented through the following sequential steps:

- The material properties are first defined, including the compressive strength of concrete (f_c'), the tensile strength of the FRP reinforcement (f_f), and the modulus of elasticity of FRP (E_f).
- The cross-sectional geometry is then specified by defining the section width (b), total height (h), effective depth (d), and the area of FRP reinforcement (A_f).
- The ultimate compressive strain of concrete (ϵ_{cu}) is introduced to satisfy strain compatibility requirements and to describe the strain profile at the failure condition.
- The nonlinear equilibrium equation is solved iteratively using the bisection method to determine the neutral axis depth (c), where the internal compressive and tensile forces are in equilibrium as illustrated in Equation 1.

$$C_c = ab \sum_{i=1}^{n_c} f_{ci} = T_t = ab \sum_{j=1}^{n_t} f_{tj} \quad (1)$$

Where C_c and T_t are the overall compressive and tensile forces in concrete, $a (=h/n)$ is the depth of each concrete segment in compression or tension; n_c and n_t are the number of concrete segments in compression and tension, respectively; b and h are the width and depth of beam, respectively; f_{ci} and f_{tj} are the concrete compressive stress in segment i , and concrete tensile stress in segment j .

- Finally, the total moment capacity is computed by integrating the stress distribution in concrete and evaluating the FRP force contribution, then summing their moment effects about a reference axis as expressed in Equation 2.

$$M = \sum_{i=1}^{n_c} C_{ci} L_{ci} - \sum_{j=1}^{n_t} T_{tj} L_{tj} \quad (2)$$

Where L_{ci} is the lever arm for concrete compressive forces C_{ci} in segment i and L_{tj} is the lever arm for concrete tensile forces T_{tj} in segment j .

Prediction of Moment Redistribution in FRP-Reinforced Continuous Concrete Beams Using Artificial Neural Networks (ANN) Implemented in Python:

Moment redistribution is an important characteristic in continuous reinforced concrete beams, particularly in statically indeterminate structures where internal forces can shift from highly stressed sections to less stressed regions after cracking and stiffness degradation. In conventional steel-reinforced concrete beams, redistribution occurs mainly due to the ductile yielding behavior of steel reinforcement. However, in FRP-reinforced concrete beams, the redistribution mechanism is significantly different because FRP bars exhibit linear elastic behavior up to failure without yielding.

In the present study, the redistribution of moments was investigated by comparing the elastic bending moments with the ultimate moments obtained from the numerical analysis at failure. The redistribution behavior was strongly influenced by the stiffness of the beam sections, cracking development, reinforcement, and the mechanical properties of the FRP bars.

For the continuous beams analyzed, the support sections initially carried higher negative moments due to the continuity effect. As loading increased and cracking developed over the middle support, the stiffness at the hogging region gradually decreased. Consequently, part of the support moment was redistributed toward the mid-span sections, resulting in increased positive moments in the sagging regions. This behavior became more pronounced in beams with lower reinforcement ratios and lower concrete compressive strengths because of their reduced flexural stiffness after cracking as expressed in Equation 3.

$$MR\% = \frac{M_e - M_u}{M_e} \times 100 \quad (3)$$

Where M_e and M_u are the critical section elastic and ultimate moments at failure.

FRP Continuous Beams: Case Study on Moment Redistribution:

FRP-reinforced concrete beams have gained considerable attention due to their high corrosion resistance, lightweight properties, and high tensile strength. However, unlike steel reinforcement, FRP bars behave linearly elastic up to failure, which affects the moment redistribution behavior of continuous beams. This study presents a numerical investigation of moment redistribution in continuous concrete beams reinforced with GFRP and CFRP bars as shown in Figure 1. The investigated parameters include the flexural reinforcement ratio, reinforcement arrangement, and type of longitudinal reinforcement material, in addition to the serviceability performance of the beams.

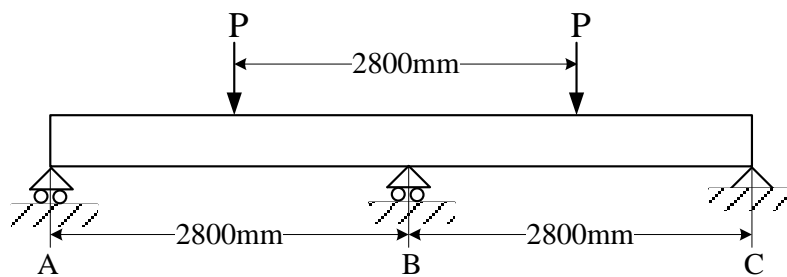


Figure (1): FRP-Reinforced Concrete Continuous Beam Subjected to Loading

1. Beam Notation:

The beams were designated according to the reinforcement condition, type of longitudinal reinforcement material, and reinforcement arrangement. For example, the notation (CB-G-UO) represents a continuous beam (CB) reinforced with GFRP bars (G), where U denotes an under-reinforced top section and O denotes an over-reinforced bottom section. Similarly, C refers to CFRP reinforcement.

The investigated parameters in this numerical study included the flexural reinforcement ratio at both sagging and hogging moment regions, as well as the type of longitudinal reinforcement material. In addition, serviceability performance was considered as a key variable in evaluating the behavior of continuous beams reinforced with FRP bars.

2. Moment Redistribution of GFRP-Reinforced Continuous Concrete Beams: A Numerical Case Study and Parametric Analysis:

This study presents a numerical case study on the moment redistribution behavior of GFRP-reinforced continuous concrete beams as illustrated in Table 1 and Figure 2. Due to the linear elastic behavior of GFRP bars up to failure, the structural response differs significantly from conventional steel-reinforced beams, particularly in terms of stiffness and redistribution capacity. A parametric analysis is conducted to evaluate the influence of flexural reinforcement ratio in sagging and hogging regions, reinforcement arrangement, and serviceability performance. The results provide insight into the structural behavior of continuous beams reinforced with GFRP under different design conditions.

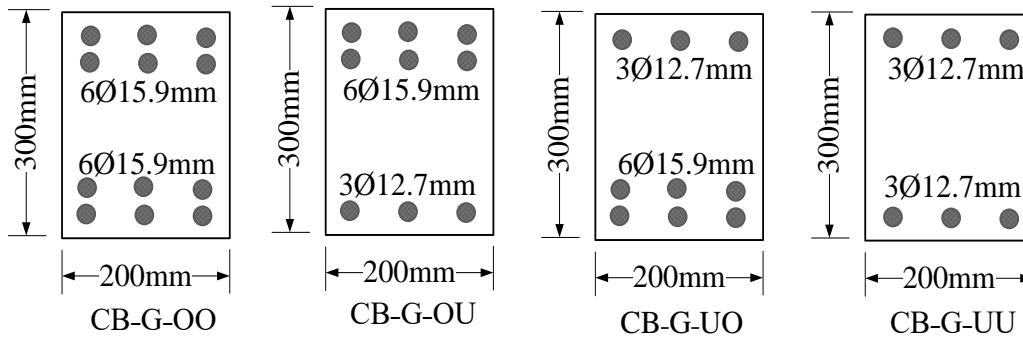


Figure (2): Reinforcement Details and Configurations of GFRP- Concrete Beams.

Table (1): Details of GFRP-Reinforced Concrete Continuous Beams.

Beam	Span (mm)	Cross Section (mm×mm)	Reinforcement		E _f (kN/mm ²)	f _c ' (N/mm ²)
			Top	Bottom		
CB-G-OO	2800	200×300	6Ø15.9	6Ø15.9	46 (Ø15.9), 44.2(Ø12.7)	40
CB-G-OU			6Ø15.9	3Ø12.7		
CB-G-UO			3Ø12.7	6Ø15.9		
CB-G-UU			3Ø12.7	3Ø12.7		

Table 2 presents the numerical ultimate moments at failure, ultimate loads, elastic moments, and the corresponding moment redistribution ratios for GFRP-reinforced continuous concrete beams with a cross section of 200mm× 300mm and concrete compressive strength of $f_c' = 40\text{MPa}$. The results further extend the observed trends from lower concrete strength levels and confirm that moment redistribution in GFRP-reinforced beams is primarily governed by reinforcement configuration and stiffness distribution, rather than by concrete strength alone. The relative difference between the ultimate moments at these critical sections remains strongly dependent on the reinforcement layout. Beams with unbalanced reinforcement configurations (CB-G-UO and CB-G-OU) exhibit distinct flexural capacities at the middle support and midspan, while beams with balanced or uniformly distributed reinforcement (CB-G-OO and CB-G-UU) develop similar ultimate moments at both locations as showed in Figures 3 and 4. A comparison between elastic moments and numerical ultimate moments indicates that, in all beams, failure occurs prior to reaching the elastic moment capacity. This response is characteristic of GFRP-reinforced concrete members, where the linear-elastic behavior of the reinforcement and limited concrete strain capacity result in brittle failure without the formation of plastic hinges. As a result, moment redistribution occurs as a consequence of cracking-induced stiffness degradation rather than ductility-driven mechanisms. The results clearly show that the redistribution behavior is governed by the variation in flexural capacity between the support and midspan regions. Beam CB-G-OO, with equal ultimate moments 124. 05kN.m at both middle support and midspan (load 265.82kN), exhibited relatively balanced behavior, with redistribution values 11.4% at middle support and -6.8% at midspan. A similar response was observed in beam CB-G-UU, where equal moments 77. 9kN.m at both sections and load 166. 93kN.m resulted in redistribution values 11.4% at middle support and -6.8% at midspan. In beam CB-G-OU, the higher support capacity 124. 05kN.m compared to 77. 9kN.m at midspan led to redistribution values -17.9% at middle support and 10.7% at midspan (load 199.89kN), indicating a shift of internal moments toward the span. Conversely, beam CB-G-UO, with lower support capacity 77. 9kN.m and higher midspan capacity 124. 05kN.m (load 232.85kN), showed the opposite trend, with a significant increase in redistribution at the support 36.4% and a reduction at midspan -21.9%.

Overall, the results confirm that moment redistribution ranges between -21.9% and 36.4% and is strongly dependent on the imbalance of flexural resistance between critical sections, where stronger regions attract higher internal moments while weaker regions experience reduced demand.

Table (2): Numerical Ultimate and Elastic Moments with Moment Redistribution for GFRP-Reinforced Concrete Continuous Beams.

Beam	Numerical ultimate moment at failure, M_u (kN. m)		P_u (kN)	Elastic moment, M_e (kN.m)		Moment redistribution, MR (%)	
	Middle support	Midspan		Middle support	Midspan	Middle support	Midspan
CB-G-OO	124.05	124.05	265.82	140	116.1	11.4	-6.8
CB-G-OU	124.05	77.9	199.89	105.2	87.3	-17.9	10.7
CB-G-UO	77.9	124.05	232.85	122.5	101.7	36.4	-21.9
CB-G-UU	77.9	77.9	166.93	87.9	72.9	11.4	-6.8

$P_u=(2/L) (M_u, \text{ at middle support } +2M_u, \text{ at midspan})$, $M_e=(0.188LP_u)$ for middle support, $M_e=(0.156LP_u)$ for midspan.

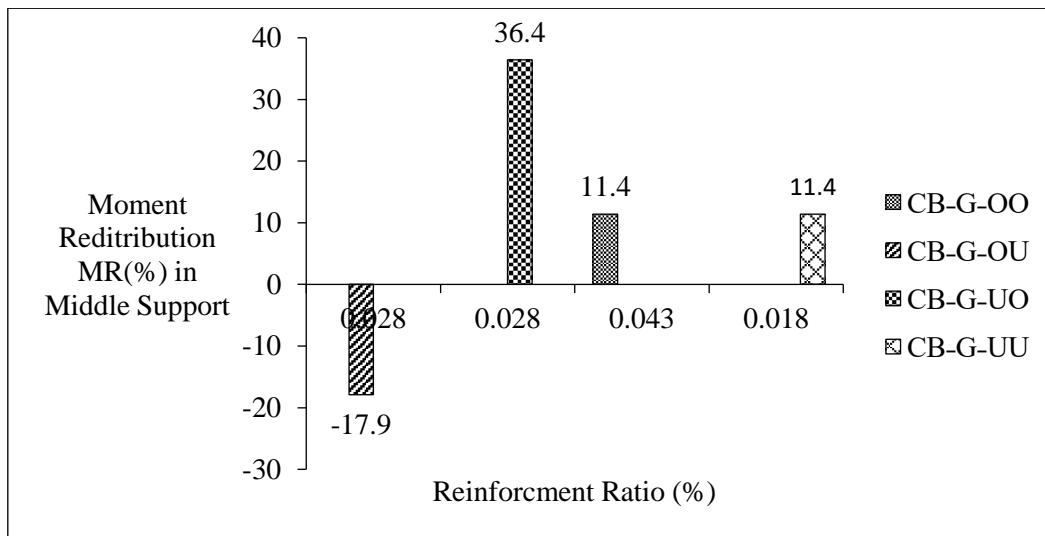


Figure (3): Moment Redistribution (MR) at Middle Support vs. Reinforcement Ratio (ρ) for GFRP-Reinforced Concrete Beams.

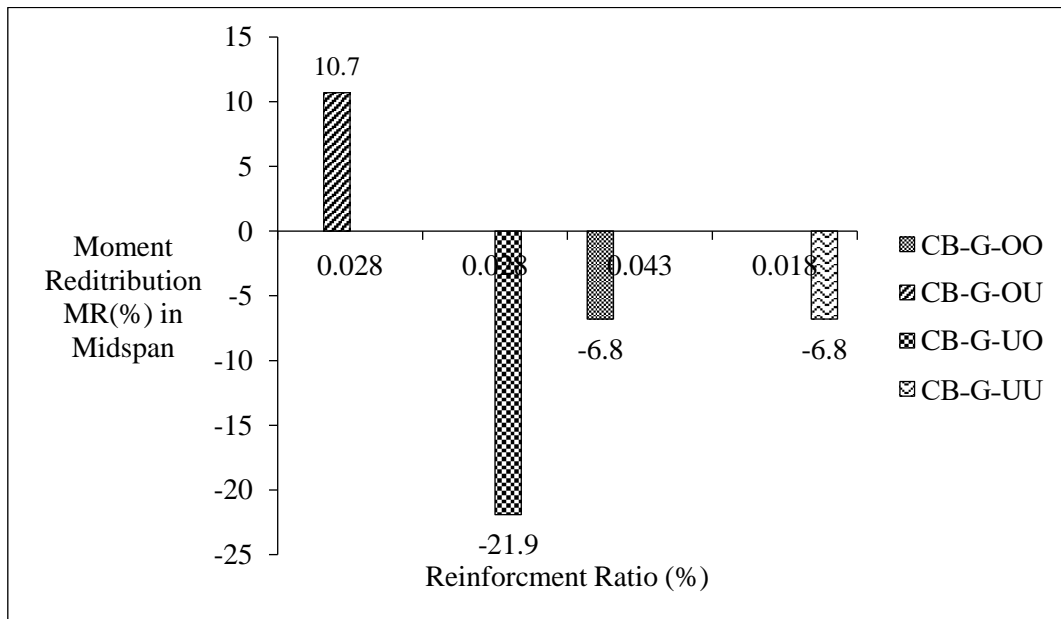


Figure (4): Moment Redistribution (MR) at Midspan vs. Reinforcement Ratio (ρ) for GFRP-Reinforced Concrete Beams.

3. Moment Redistribution of CFRP-Reinforced Continuous Concrete Beams: A Numerical Case Study and Parametric Analysis:

This section presents a numerical case study on the moment redistribution behavior of CFRP-reinforced continuous concrete beams as presented in Table 3 and Figure 5. Due to the linear elastic behavior and high strength of Carbon Fiber Reinforced Polymer (CFRP) bars, the structural response and redistribution capacity differ from conventional steel-reinforced members. A parametric analysis is performed to study the influence of flexural reinforcement ratio in sagging and hogging regions, reinforcement arrangement, and serviceability performance. The results highlight the effect of CFRP reinforcement on the overall behavior of continuous concrete beams.

Table (3): Details of CFRP-Reinforced Concrete Continuous Beams.

Beam	Span (mm)	Cross section (mm×mm)	Reinforcement		E_f (kN/mm ²)	f_c' (N/mm ²)
			Top	Bottom		
CB-C-OO	2800	200×300	3Ø12mm	3Ø12mm	200	40
CB-C-UO			2Ø7.5mm	3Ø12mm		
CB-C-OU			3Ø12mm	2Ø7.5mm		
CB-C-UU			2Ø7.5mm	2Ø7.5mm		

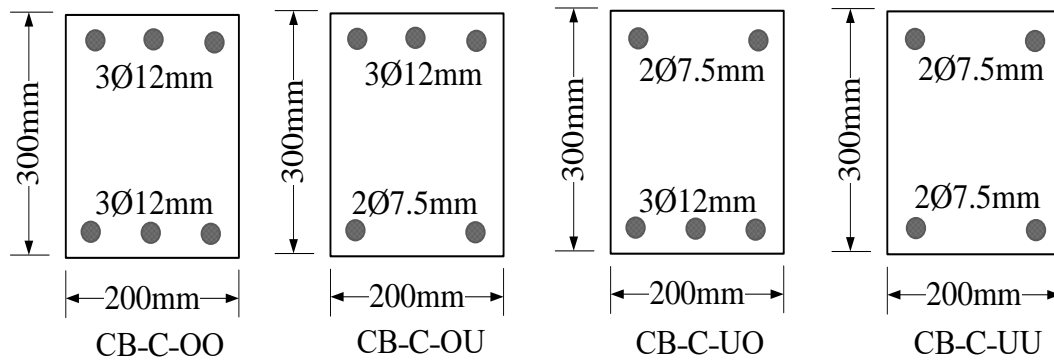


Figure (5): Reinforcement Details and Configurations of CFRP- Concrete Beams.

Table 4 presents the numerical ultimate moments, ultimate loads, elastic moments, and moment redistribution ratios for CFRP-reinforced continuous concrete beams. The results clearly demonstrate that the redistribution mechanism is strongly governed by the relative flexural capacity between the support and midspan sections as shown in Figures 6 and 7. Beam CB-C-OO, characterized by equal ultimate moments of 83. 4kN.m at both support and midspan and an ultimate load of 178.7kN, exhibited a nearly symmetric structural response. The corresponding redistribution values were 11.3% at the support and approximately -6.9% at midspan. Similarly, beam CB-C-UU, with equal ultimate moments of 35. 9kN.m at both critical sections and a load of 76.9kN, showed comparable behavior, with 11.3% redistribution at the support and approximately -6.8% at midspan, confirming the influence of symmetric reinforcement on stabilizing internal force distribution. In contrast, beam CB-C-OU, where the support capacity (83. 4kN.m) exceeded the midspan capacity (35. 9kN.m), exhibited a pronounced redistribution effect. The redistribution increased to 52.8% at the support and decreased to -31.9% at midspan (ultimate load 110.8kN), indicating a clear transfer of internal moments toward the weaker span region. Conversely, beam CB-C-UO, with higher midspan capacity (83. 4kN.m) and lower support capacity (35. 9kN.m), showed the opposite trend. The redistribution reached -43% at the support and 25.8% at midspan (ultimate load 144.7kN), reflecting significant moment transfer toward the support region.

Overall, the redistribution values ranging from -43% to 52.8% highlight the strong sensitivity of CFRP-reinforced continuous beams to reinforcement configuration, where imbalance in flexural stiffness governs both the direction and magnitude of moment redistribution.

Table (5): Numerical Ultimate and Elastic Moments with Moment Redistribution for CFRP-Reinforced Concrete Continuous Beams.

Beam	Numerical ultimate moment at failure, M_u (kN.m)		P_u (kN)	Elastic moment, M_e (kN.m)		Moment redistribution, MR (%)	
	Middle support	midspan		Middle support	midspan	Middle support	midspan
CB-C-OO	83.4	83.4	178.7	94	78	11.3	-6.9
CB-C-OU	83.4	35.9	110.8	76.17	63.2	52.8	-31.9
CB-C-UO	35.9	83.4	144.7	58.3	48.4	-43	25.8
CB-C-UU	35.9	35.9	76.9	40.5	33.6	11.3	-6.8

$P_u=(2/L) (M_u, \text{ at middle support } +2M_u, \text{ at midspan}), M_e=(0.188LP_u) \text{ for middle support, } M_e=(0.156LP_u) \text{ for midspan.}$

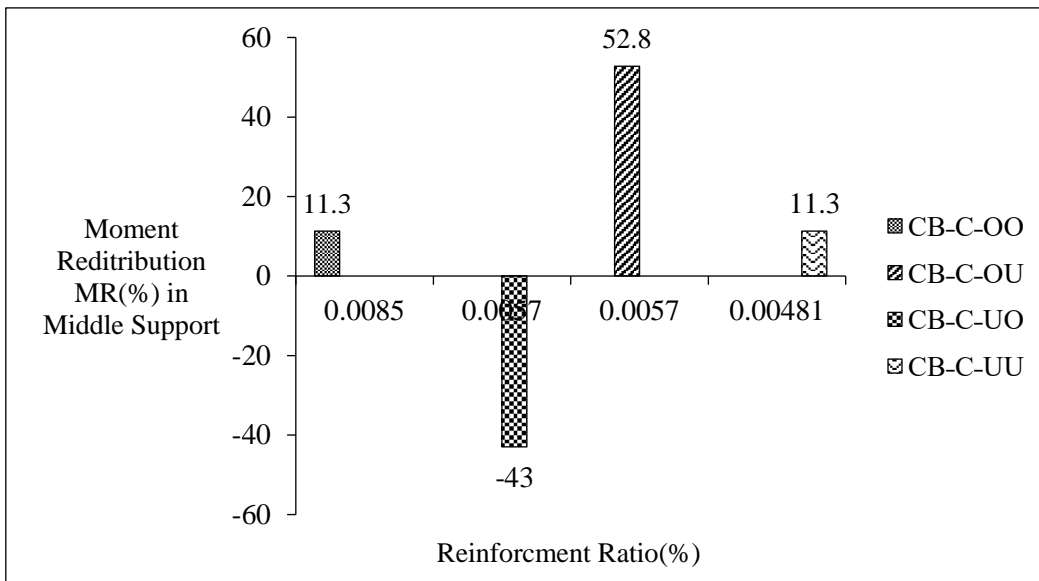


Figure (6): Moment Redistribution (MR) at Middle Support vs. Reinforcement Ratio (ρ) for CFRP-Reinforced Concrete Beams.

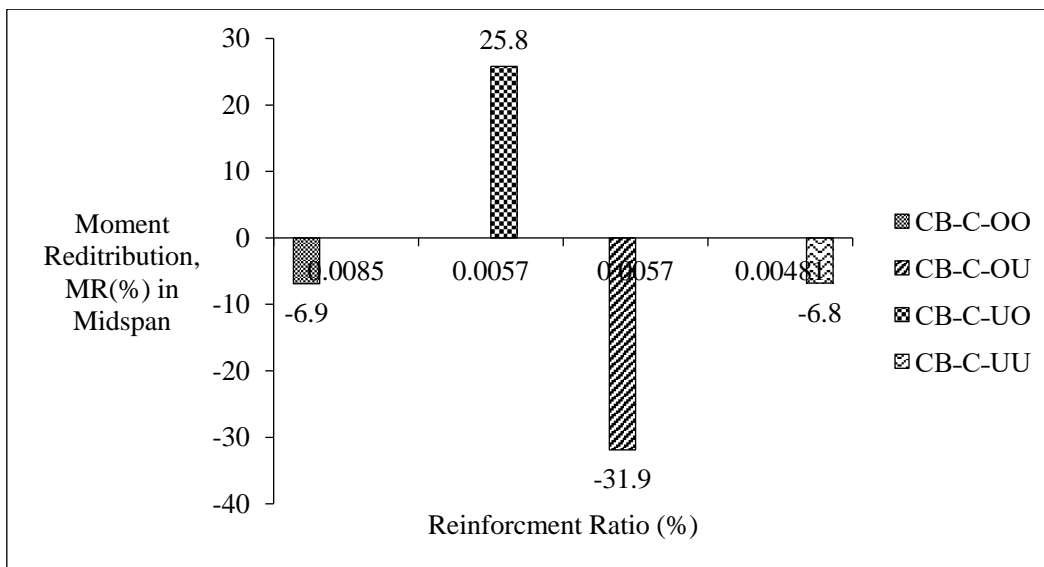


Figure (7): Moment Redistribution (MR) at Midspan vs. Reinforcement Ratio (ρ) for CFRP-Reinforced Concrete Beams.

Conclusion:

This study investigated the flexural behavior and moment redistribution of continuous CFRP and GFRP reinforced concrete beams with different reinforcement arrangements. The numerical results clearly demonstrate that both ultimate capacity and redistribution behavior are strongly governed by the distribution of reinforcement between the support and midspan regions. For CFRP beams, the ultimate moment at the critical sections varied between 35.9 kN·m and 83.4 kN·m, while the ultimate load ranged from 76.9 kN to 178.7 kN. The elastic moments were in the range of 33.6 kN·m to 94 kN·m. The moment redistribution exhibited a wide variation from -43% to 52.8%, with the highest redistribution occurring in asymmetric configurations where a strong imbalance exists between support and span capacities. For GFRP beams, the ultimate moment ranged from 77.9 to 124.05 kN·m, with corresponding ultimate loads between 190.7 kN and 265.82 kN. The elastic moments varied from 72.9 to 116.1 kN·m, while the moment redistribution ranged from -21.9% to 36.4%, indicating a relatively more moderate redistribution response compared to CFRP beams. The results also show that symmetric reinforcement configurations (OO and UU cases) generally lead to balanced structural response with low redistribution levels (approximately -6.9% to 11%). In contrast, asymmetric configurations (OU and UO cases) produce significant moment transfer between support and midspan, where stronger sections attract higher internal forces and weaker sections experience reduced or reversed redistribution.

Overall, the study confirms that moment redistribution in FRP-reinforced continuous beams is primarily controlled by sectional stiffness, reinforcement arrangement, and cracking behavior rather than ductility. These findings highlight the importance of achieving a balanced reinforcement distribution to ensure stable structural performance and controlled internal force redistribution in design practice.

References:

1. American Concrete Institute (2015). Guide for the Design and Construction of Structural Concrete Reinforced with FRP Bars (ACI 440.1R-15). American Concrete Institute.
2. Bank, Lawrence C. (2006). Composites for Construction: Structural Design with FRP Materials. John Wiley & Sons.
3. Mohamed Elarbi Mahroug (2026). "Accuracy Assessment of Python- Implemented Artificial Intelligence Models for Predicting Moment Capacity of FRP Reinforced concrete Beams." International Science and Technology Journal, 38(2).
4. Benmokrane, Brahim, Chaallal, O., and Masmoudi, R. (2002). "Glass Fibre Reinforced Plastic (GFRP) Rebars for Concrete Structures." Construction and Building Materials, 9(6), 353–364.
5. El-Salakawy, Ehab, Benmokrane, B., and Desgagné, G. (2003). "FRP Reinforced Concrete Slabs under Concentrated Loads." Journal of Composites for Construction, 7(3), 184–191.
6. Grace, Nabil F., Soliman, A. K., Abdel-Sayed, G., and Saleh, K. R. (1998). "Behavior and Ductility of Simple and Continuous FRP Reinforced Beams." Journal of Composites for Construction, 2(4), 186–194.
7. Gravina, Ricardo J. and Smith, S. T. (2008). "Flexural Behavior of Indeterminate Concrete Beams Reinforced with FRP Bars." Engineering Structures, 30(9), 2370–2380.
8. Habeeb, M. N. and Ashour, A. F. (2008). "Flexural Behavior of Continuous GFRP Reinforced Concrete Beams." Journal of Composites for Construction, 12(2), 115–124.
9. Mehta, P. Kumar and Monteiro, P. J. M. (2014). Concrete: Microstructure, Properties, and Materials. McGraw-Hill Education.
10. Neville, Adam M. (2011). Properties of Concrete. Pearson Education Limited.
11. Ospina, Carlos E. and Gross, S. P. (2005). "Moment Redistribution in FRP Reinforced Concrete Continuous Beams." ACI Structural Journal, 102(2), 203–211.
12. Toutanji, Houssam and Saafi, M. (2000). "Flexural Behavior of Concrete Beams Reinforced with Glass Fiber Reinforced Polymer (GFRP) Bars." ACI Structural Journal, 97(5), 712–719.